

Supporting Information

A Water-Soluble NIR-II Fluorescent Probe for Non-Invasive Real-Time Detection of Blood ATP via Optoacoustic and Fluorescence Imaging

Yonghe Zhang, Fang Zeng*, and Shuizhu Wu*

State Key Laboratory of Luminescent Materials and Devices, Guangdong Provincial Key Laboratory of Luminescence from Molecular Aggregates, College of Materials Science and Engineering, South China University of Technology, Guangzhou 510640, China

[*] Corresponding authors

E-mail: mcfzeng@scut.edu.cn

shzhwu@scut.edu.cn

Contents

General experimental procedures	3
Figure S1	8
Figure S2.....	9
Figure S3.....	9
Figure S4.....	10
Figure S5.....	10
Figure S6.....	11
Figure S7.....	11
Figure S8	12
Figure S9.....	13
Figure S10.....	13
Figure S11.....	14
Figure S12.....	14
Figure S13.....	15
Figure S14.....	16
Figure S15.....	17
Figure S16.....	18
Table S1.....	19
References:	21

General experimental procedures

1. Reagents

Sodium hydroxide, sodium acetate, 1,1,2-trimethylbenz[e]indole, P-toluenesulfonyl chloride and phosphorus oxychloride were purchased from Energy Chemical Reagents. 2,2' -Dipyridine methylamine, 4,4-dimethylcyclohexanone, nonaethylene glycol monomethyl ether were purchased from Shanghai Bide Medical Technology Co., Ltd. The solvents including tetrahydrofuran (THF), N, N-dimethylformamide (DMF), triethylamine (TEA), acetic anhydride, toluene (Tol) and dichloromethane (DCM) were analytical grade reagents. The water used in the experiments was deionized water.

2. Apparatus

Nuclear magnetic resonance (NMR) spectra were measured on Bruker AVANCE 400 MHz NMR spectrometer. ^1H NMR and ^{13}C NMR were conducted at 400 MHz and 101 MHz respectively. High resolution mass spectrometer (HR-MS) was recorded on a Bruker MAXIS IMPACT mass spectrometer. The Near-Infrared-II (NIR-II) fluorescence spectra were measured on NIRQUEST512 spectrometer (Ocean Optics, USA. Excitation: 808 nm laser, emission range: 900-1700 nm). The absorption spectra were collected on Hitachi U-3010 absorption spectrophotometer. The NIR-II fluorescence (in vivo and ex vivo) imaging was conducted on NIR-II in Vivo Fluorescent Imaging System (Series II 808/900-1700, Suzhou NIR-Optics Technologies Co., Ltd.). Optoacoustic imaging was performed using inVision128 multispectral optoacoustic tomographic (MSOT) imaging system (iThera Medical GmbH) equipped with viewMSOT 4.0 for data processing.

3. Synthesis

Nonaethylene glycol monomethyl ether and sodium hydroxide were placed in a two-mouth flask. THF/ H_2O was added to the flask at 0 °C. Then, p-toluenesulfonyl chloride was dissolved in 7 mL THF and added to the flask through a constant pressure drip funnel. The solution was kept under stirring for 2 hours, and then the mixture was placed at room temperature and kept under stirring for 12 hours. The reaction solution was extracted with DCM, dried with anhydrous sodium sulfate, and the solvents were removed under reduced pressure. Compound 1 (white product) was obtained without further purification.

Compound 1 was dissolved in toluene with 1,1, 2-trimethyl-1H-benzo [e] indole and reacted for 10 h at 120 °C under N₂. At the end of the reaction, the crude was washed with hexane, and the solvents were removed under reduced pressure under reduced pressure. Compound 2 (purple oily liquid) was obtained without further purification.

Phosphorus oxychloride was dissolved in the mixture of DCM and DMF, and then 4, 4-dimethylcyclohexanone was dissolved in the mixture, and the reaction was lasted for 4 h. The reaction solution was poured into an ice water bath, and the solid was precipitated, it was filtered, and compound 3 (Orange solid) was obtained.

HC9: Compound 2 (1.50 g, 2.41 mmol) and compound 3(0.24 g, 1.2 mmol) were dissolved in acetic anhydride with sodium acetate and reacted for 1.5 h under N₂. Purification was performed by column chromatography with the eluent DCM : MeOH (v : v = 14 : 1). HC9 (green oily product) was obtained (Yield: 75%, 1.26 g). ¹H NMR (400 MHz, CDCl₃) δ (ppm): 8.48 (s, 2H) 8.13 (s, 2H), 7.94 (s, 2H), 7.71-7.69 (t, *J* = 8 Hz, 2H), 7.61 (s, 2H), 7.54-7.52 (t, *J* = 8 Hz, 2H), 4.23-4.20 (t, *J* = 8 Hz, 4H), 3.65-3.49 (m, 68H), 3.37 (s, 6H), 1.70-1.67 (t, *J* = 8 Hz, 4H), 1.42-1.39 (t, *J* = 8 Hz, 4H), 1.34-1.28 (m, 12H), 1.17 (s, 6H).

HCD9: HC9(1.00 g, 0.711 mmol) and 2,2'-dipyridine methylamine (0.17 g, 0.853 mmol) were dissolved in a mixed solution of DMF and TEA and reacted for 5 h under N₂. The crude product was purified by column chromatography with the eluent DCM : MeOH (v : v = 13 : 1). HCD9 (blue oily product) was obtained (Yield: 65%, 0.72 g). ¹H NMR (400 MHz, CDCl₃) δ (ppm): 8.57 (s, 2H), 7.92-7.79 (m, 4H), 7.69-7.66 (t, *J* = 8Hz, 4H), 7.46-7.41 (m, 2H), 7.38-7.36 (d, *J* = 8Hz, 4H), 7.21-7.19 (t, *J* = 4Hz, 4H), 4.34-4.32 (t, *J* = 4 Hz, 2H), 4.10 (s, 2H), 3.93-3.91 (t, *J* = 4Hz, 2H), 3.73-3.53 (m, 68H), 3.37-3.36 (d, *J* = 4Hz, 6H), 2.01 (s, 4H), 1.74 (s, 4H), 1.25 (s, 12H), 1.13-1.10 (d, *J* = 8Hz, 3H), 0.88-0.86 (t, *J* = 4Hz, 3H). ¹³C NMR (126 MHz, CDCl₃) δ 171.65, 158.55, 150.22, 149.37, 143.71, 140.65, 137.57, 136.62, 131.37, 130.23, 124.36, 123.99, 123.15, 122.40, 122.22, 71.49, 71.05, 70.61, 70.56, 70.52, 70.48, 70.45, 68.03, 60.70, 59.04, 54.29, 53.43, 50.05, 44.08, 40.40, 29.41, 28.19.

The HCD9 HRMS: calcd. for [C₉₀H₁₂₈N₅O₁₈]⁺ [M]⁺: m/z 1566.9249; Found: 1566.9282. The HCD9-Zn[II] HRMS: calcd. for [C₉₀H₁₂₈N₅O₁₈Zn]³⁺ [M]³⁺: m/z 543.6177; Found: 543.6178.

4. Preparation of the HCD9-Zn[II] complex

The HCD9-Zn[II] complex was synthesized by stirring a 1 : 1.2 molar mixture of HCD9 and zinc chloride in water for 3 hours.

5. Determination of the detection limit

The detection limit was determined based on the fluorescence titration experiment. The fluorescence emission spectra of the probe HCD9-Zn[II] were measured ten times and the standard deviation of blank measurement was obtained. In addition, the fluorescence intensity (at 924 nm) was plotted against the increasing concentrations of ATP. Then the detection limit was calculated with the following equation:

$$\text{Detection Limit} = 3\sigma/\kappa$$

Where σ is the standard deviation of blank measurement, κ is the slope between the fluorescence intensity ratios versus the concentrations of ATP.

6. Cell experiments

L929 cells were purchased from KeyGEN BioTECH Co., Ltd. and cultured in Dulbecco's modified Eagle's medium (DMEM) containing 10% (v/v) bovine serum. Cell incubator was maintained at 37 °C and a humidified 5% CO₂ atmosphere. The cytotoxicity of HCD9 and HCD9-Zn[II] was evaluated on L929 cells by standard methyl thiazolyl tetrazolium (MTT) assay. Briefly, cells were seeded into 96-well plates at the cell density of 5000 cells per well and cultured for 24 h. Then, the medium in all wells was replaced with fresh ones containing different concentrations of the HCD9 and HCD9-Zn[II] (0, 5, 10, 20, 30, 40, 50, 60 and 70 μM) and the cells were cultured for another 24 h. After that, MTT (0.5 mg mL⁻¹) was added to the culture medium in each well and incubated for an additional 4 h. Finally, each well was washed with sterile PBS for 3 times and the medium was replaced with 150 μL DMSO to dissolve the precipitates. The optical density at 570 nm for each well was measured by Thermo MK3 ELISA reader to access cell viability. Three independent experiments were conducted for each concentration and 8 replicates were performed in each independent experiment.

7. Tissue histological evaluation

For biosafety evaluation, the healthy mice were i.v. injected with saline (100 μL) or HCD9-Zn[II] (3.2 mg kg⁻¹, in 100 μL saline) daily. After 7 days, the mice were euthanized to dissect the major organs (including hearts, livers, spleens, lungs and kidneys), the organs were fixed with 10% paraffin and embedded in paraffin wax. After that, the embedded tissue samples were sectioned for hematoxylin and eosin (H&E) staining analyses.

8. Hemolysis assay

Blood was collected from mice, and erythrocytes were isolated by centrifugation of whole blood diluted in sterile saline at 1500 rpm for 10 minutes. The supernatant was discarded, and the erythrocytes were washed three times with sterile saline. The washed red blood cells (RBCs) were then resuspended in sterile saline to a final concentration of 5%.

For the experimental groups, RBCs suspensions were incubated with either HCD9 or HCD9-Zn[II] (60 μ M). The positive control consisted of RBCs mixed with distilled water (to induce complete hemolysis), while the negative control consisted of RBCs mixed with saline (no hemolysis). All samples were incubated at 37 °C for 50 minutes. After incubation, non-hemolyzed erythrocytes were removed by centrifugation at 1500 rpm for 10 minutes. All of the readings were taken at 415 nm that is the characteristic absorption of hemoglobin. The percentage of hemolysis was calculated as follows formula: Hemolysis% = [(sample absorbance -negative control)/(positive control -negative control)] \times 100%.

9. Animal studies

Female BALB/c mice (5-6 weeks old) were provided by Guangdong Yaokang Biotechnology Co., LTD and kept in a specific-pathogen-free (SPF) animal lab at the Laboratory Animal Center of South China Agricultural University under standard care. Mice were allowed free access to SPF diet and sterile water and kept at a 12/12 h light/dark cycle.

All in vivo experiments were approved by and conducted in accordance with the guidelines of the Ethics Committee of Laboratory Animal Center of South China Agricultural University (Approval No. 2025D002). This study was conducted in conformity with the Regulations on the Administration of Laboratory Animals of Guangdong Province and the National Regulations on the Management of Laboratory Animals of China.

Experimental design:

For the experiments, healthy mice were randomly divided into 3 mice per group (n = 3 per group). The control group received no ATP, while three experimental groups were administered different doses of ATP via intravenous injection: Group 1: 0.5 mg kg⁻¹, Group 2: 1.1 mg kg⁻¹, Group 3: 2.2 mg kg⁻¹. ATP was dissolved in saline before administration. One minute after ATP administration, HCD9-Zn[II] was intravenously injected, and then in-vivo imaging was conducted.

10. In vivo imaging

For near-infrared-II (NIR-II) fluorescent imaging, an 808 nm laser was used as the excitation light with a power density of 50 mW cm⁻² on the imaging plane. Optoacoustic (OA) imaging was conducted on the inVision 128 MSOT system from iThera Medical GmbH.

The mice were intravenously (i.v.) injected with the probe HCD9-Zn(II) (3.2 mg kg⁻¹) and imaged at designated time points, which included 0, 5, 15, 25, 35, 45, 60 min for NIR-II fluorescent imaging and 5, 15, 25, 35, 45, 60 min for optoacoustic imaging. In optoacoustic imaging, the major absorbance turning points for both endogenous and exogenous photo-absorbers including 680, 700, 720, 730, 750, 760, 780, 800, 830, 860 and 900 nm were adopted as the imaging wavelengths, and 10 frames were recorded for every turning wavelength. Among the all absorbance turning points, 900 nm was selected as a background wavelength to reflect the mouse anatomy. Two-dimensional (2D) cross-sectional images were acquired at a step size of 0.5 mm covering the mice jugular veins, so that these 2D images were reconstructed into the z-stack orthogonal-view three-dimensional (3D) images. After the reconstruction, spectral unmixing was processed to separate different signals contributed from the activated probe or endogenous ones including hemoglobin.

11. Statistical analysis

As for statistical analyses of data, first the mean values and standard deviation (SD) were calculated. Then, data were presented as mean \pm SD. As for the photophysical data (fluorescence or absorption spectra), the sample size was $n = 3$ (independently performed in triplicate). As for cell viability data, the sample size was $n = 3$ (three independent experiments for each concentration with eight replicates in each independent experiment). For the data in the animal experiments, the sample size was $n = 3$.

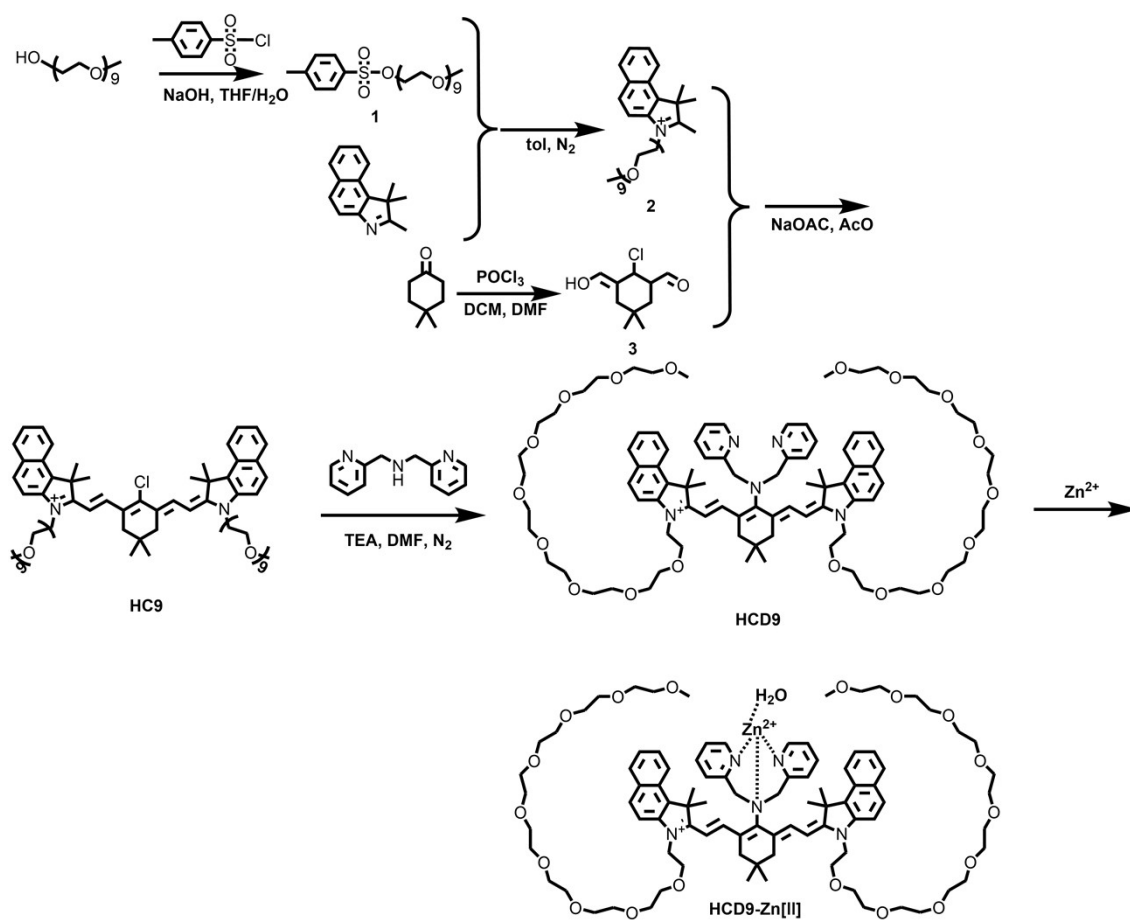


Figure S1 Synthetic route for HCD9 and HCD9-Zn[II].

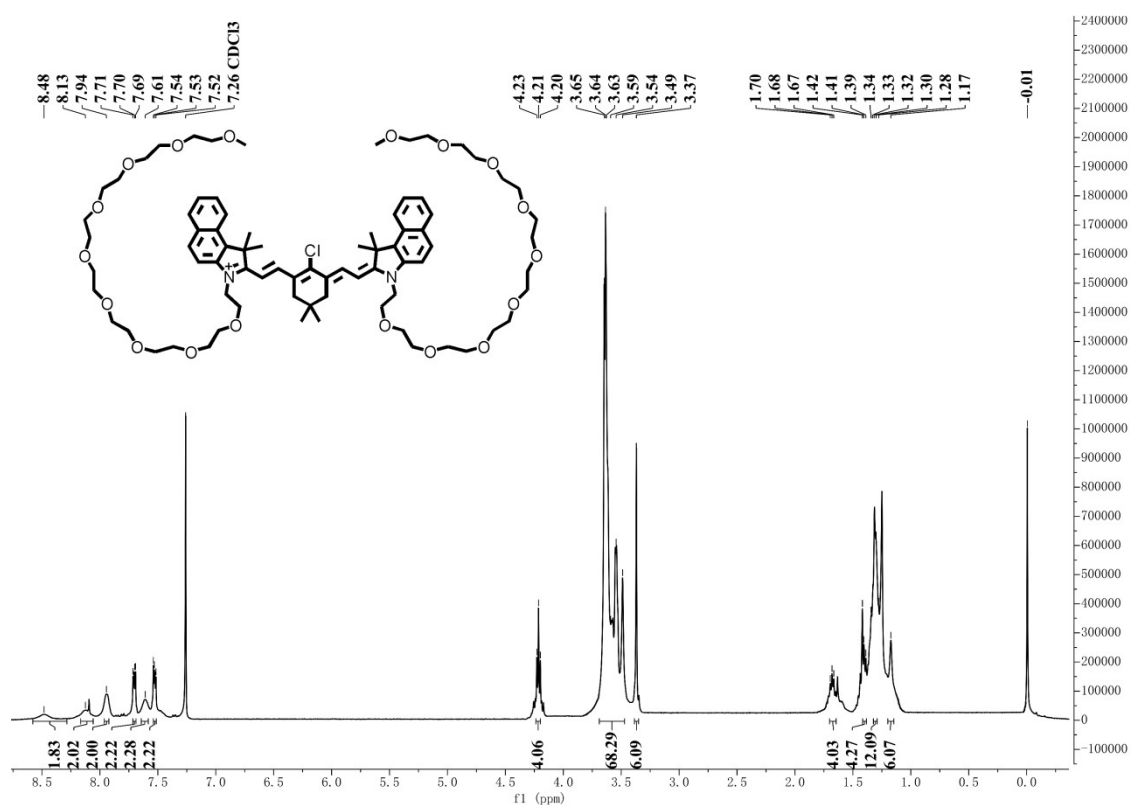


Figure S2. ^1H NMR spectrum of HC9 in CDCl_3 .

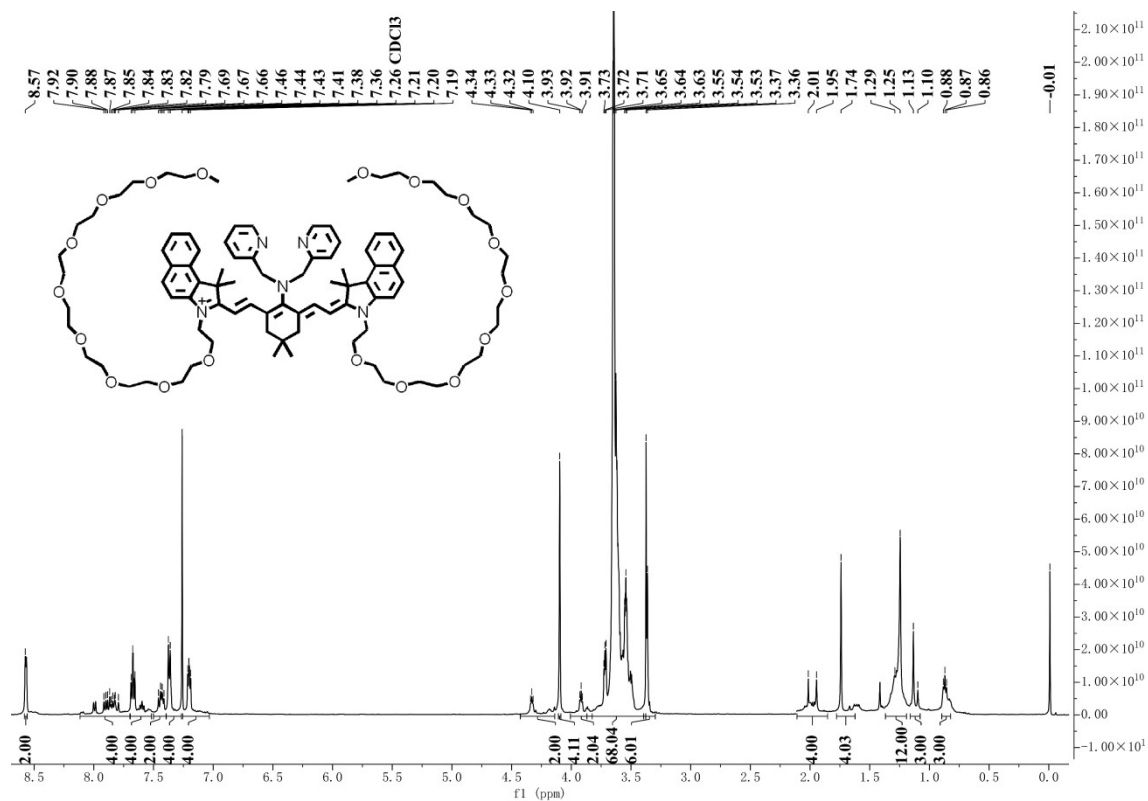


Figure S3. ^1H NMR spectrum of HCD9 in CDCl_3 .

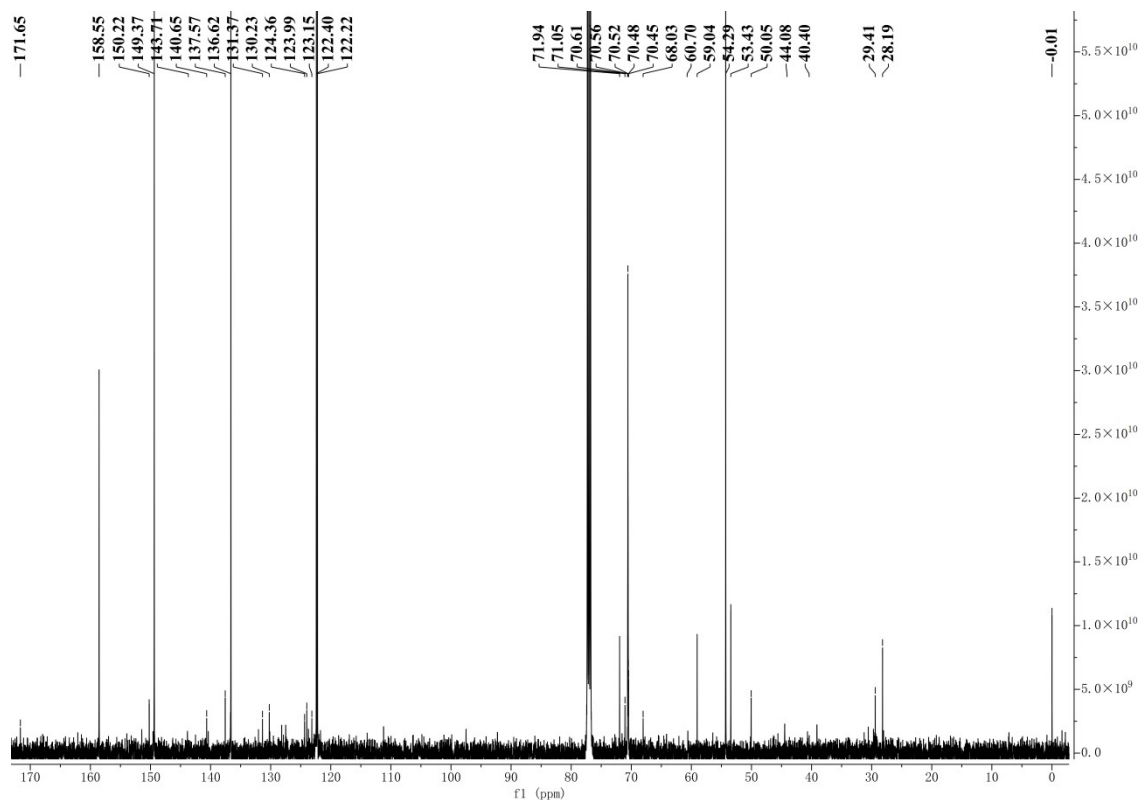


Figure S4. ¹³C NMR spectrum of HCD9 in CDCl₃.

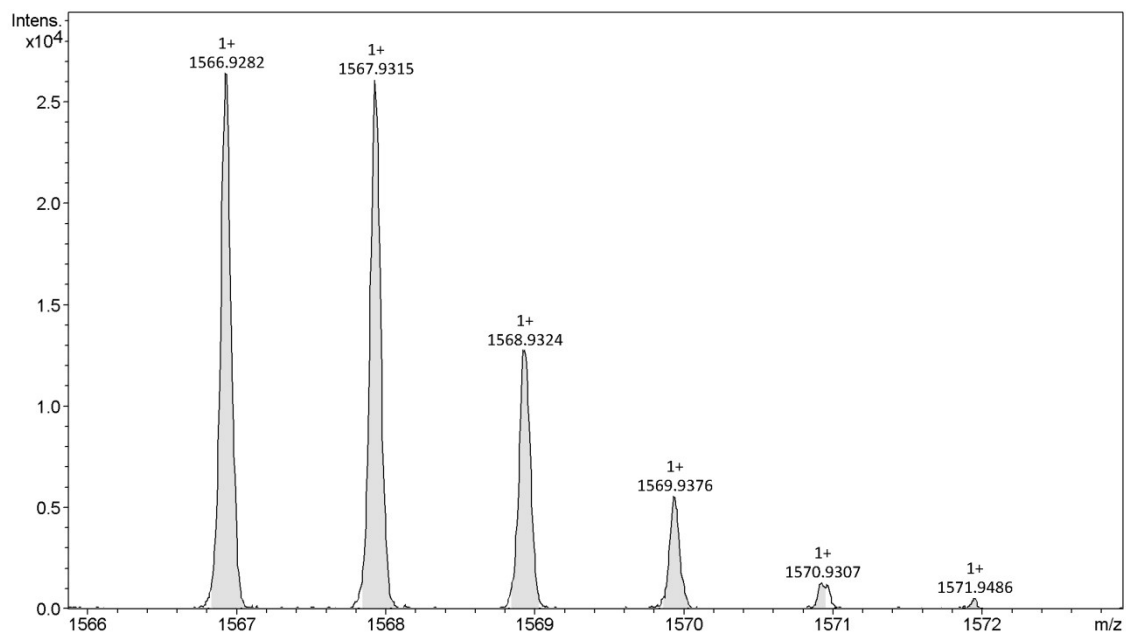


Figure S5 HR Mass spectrum of the HCD9.

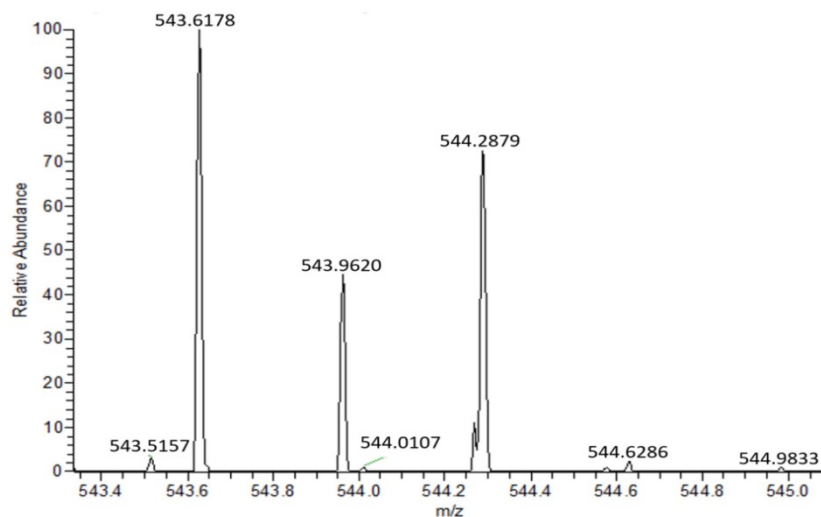


Figure S6 HR Mass spectrum of HCD9-Zn[II].

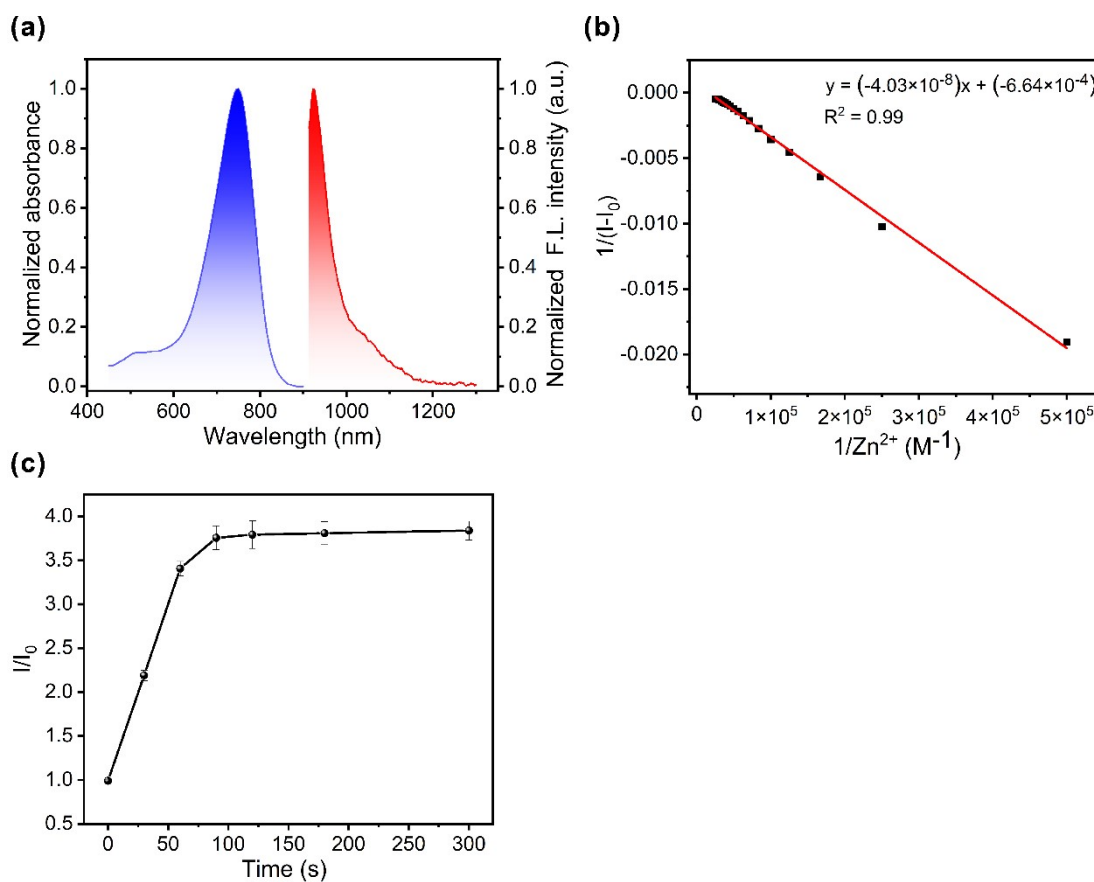


Figure S7 (a) Normalized absorption and emission spectra for HCD9 in water. (b) Determination of the binding constant of HCD9 to Zn[II]. (c) Emission intensity ratio of HCD9-Zn[II] solution before and after addition of ATP over time (I : emission intensity at 924 nm at a given time after addition of ATP into HCD9-Zn[II] solution, I_0 : emission intensity at 924 nm of HCD9-Zn[II] solution in the absence of ATP. (HCD9: 20 μ M).

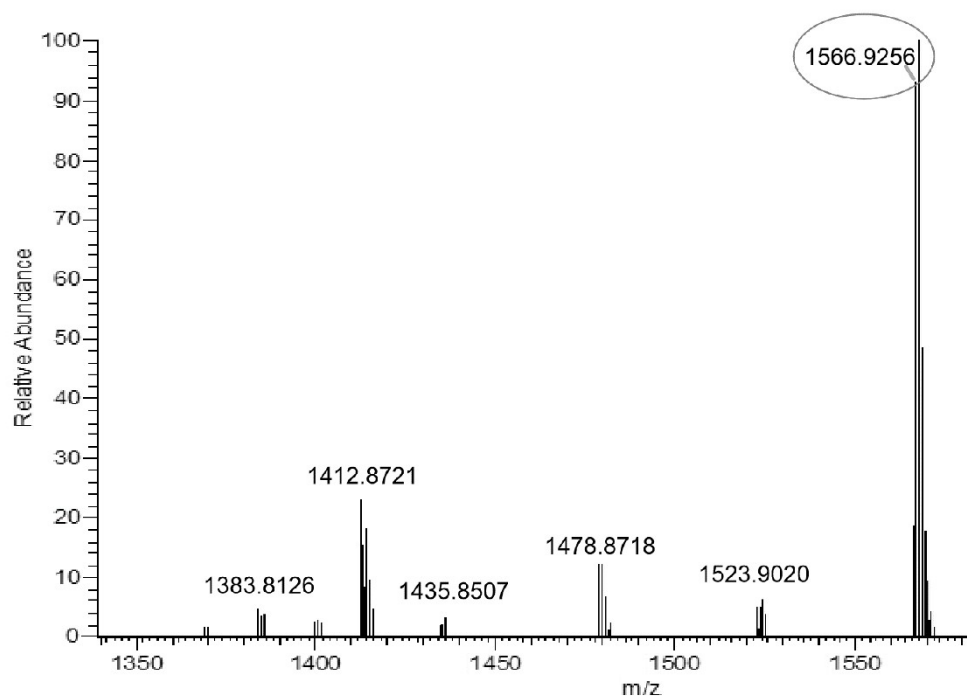


Figure S8 HR Mass spectrum of the reaction solution after the reaction between HCD9-Zn[II] and ATP

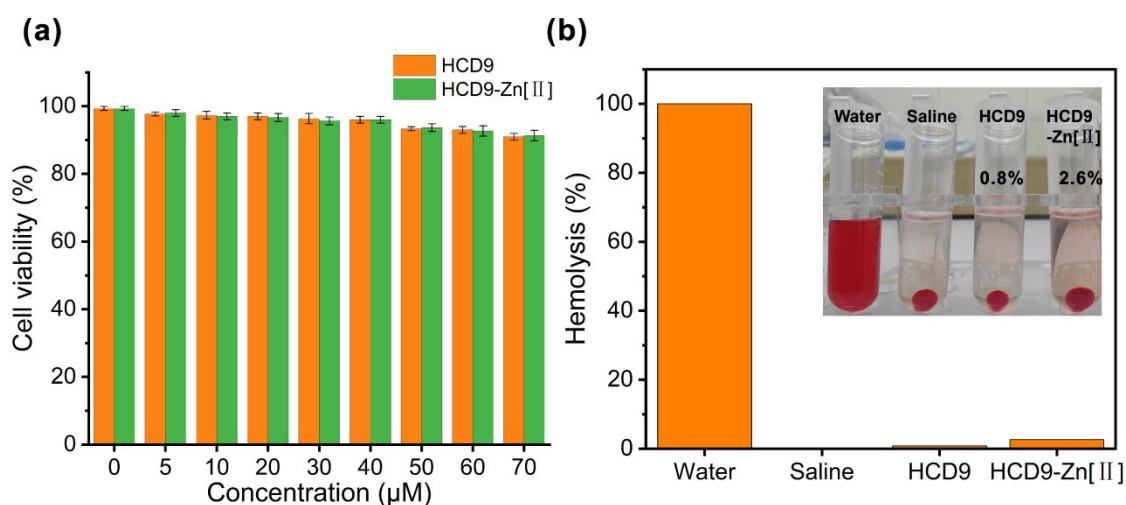


Figure S9 (a) Viabilities of L929 cells upon incubation with different concentrations of the HCD9 or HCD9-Zn[II] for 24 h by MTT assay. 3 independent experiments were conducted for each concentration and 8 replicates were performed in each independent experiment. Data represent mean \pm SD. (b) Degree of hemolysis of the HCD9 and HCD9-Zn[II] (Inset: images of red blood cells solutions after centrifugation) HCD9-Zn[II] (HCD9: 60 μ M).

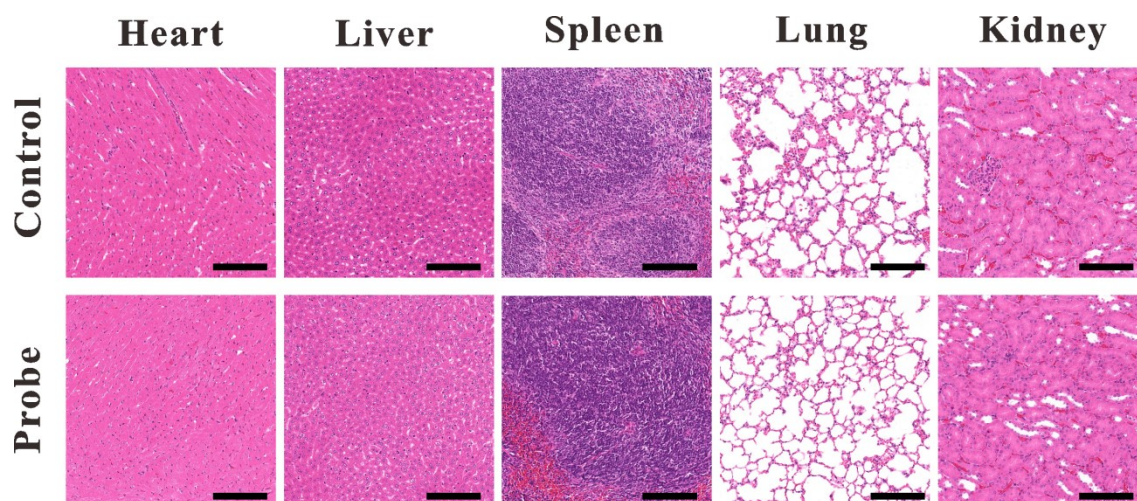


Figure S10 H&E staining analyses of the tissue sections of heart, liver, spleen, lung and kidney from the mice i.v. injected with saline (100 μ L) or HCD9-Zn[II] (3.2 mg kg⁻¹, in 100 μ L saline). Scale bar = 100 μ m.

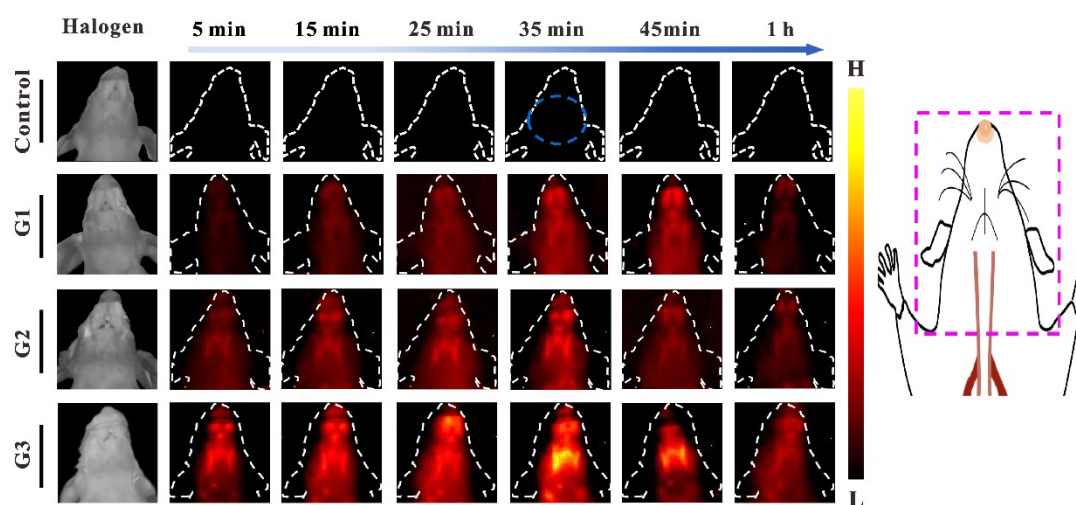


Figure S11 The NIR-II fluorescence images of the different groups of mice injected with the probe HCD9-Zn[II] (3.2 mg kg^{-1}) and after ATP pre-injection (Control: 0 mg kg^{-1} , G1: 0.5 mg kg^{-1} , G2: 1.1 mg kg^{-1} , G3: 2.2 mg kg^{-1}). (The aqua blue-circle ROI covering mice's jugular veins). Magenta dotted-line square in the mouse picture shows the imaging region in the NIR-II fluorescence imaging.

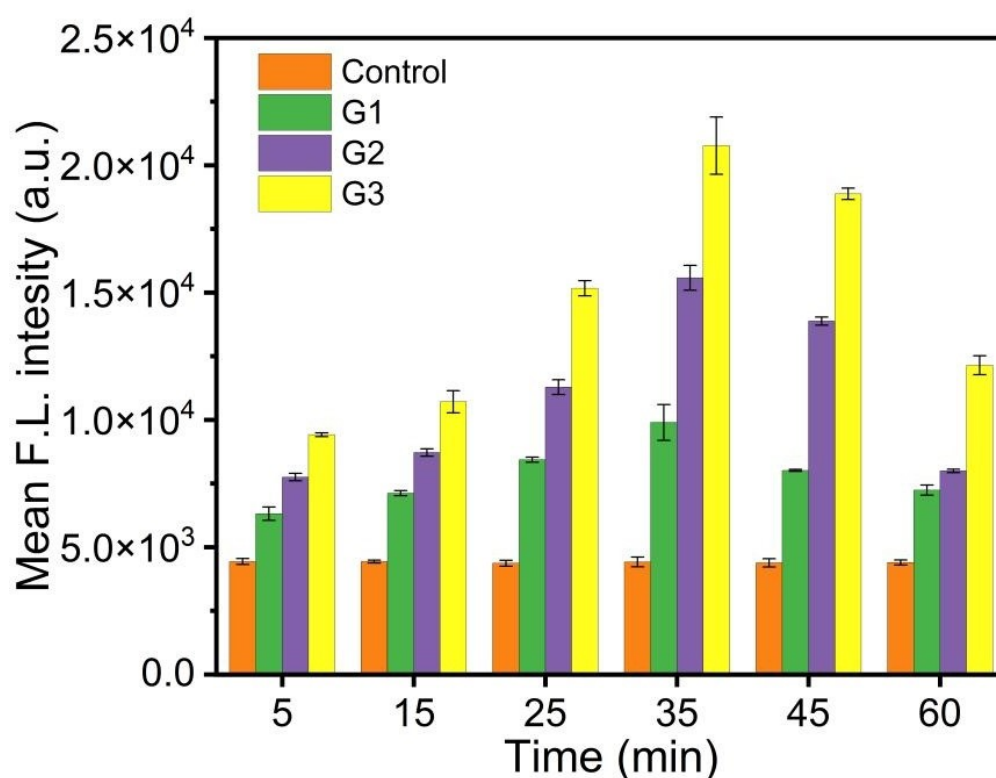


Figure S12 Mean NIR-II fluorescent intensities of the ROI covering jugular veins (the blue circle) of mice at different time (n = 3).

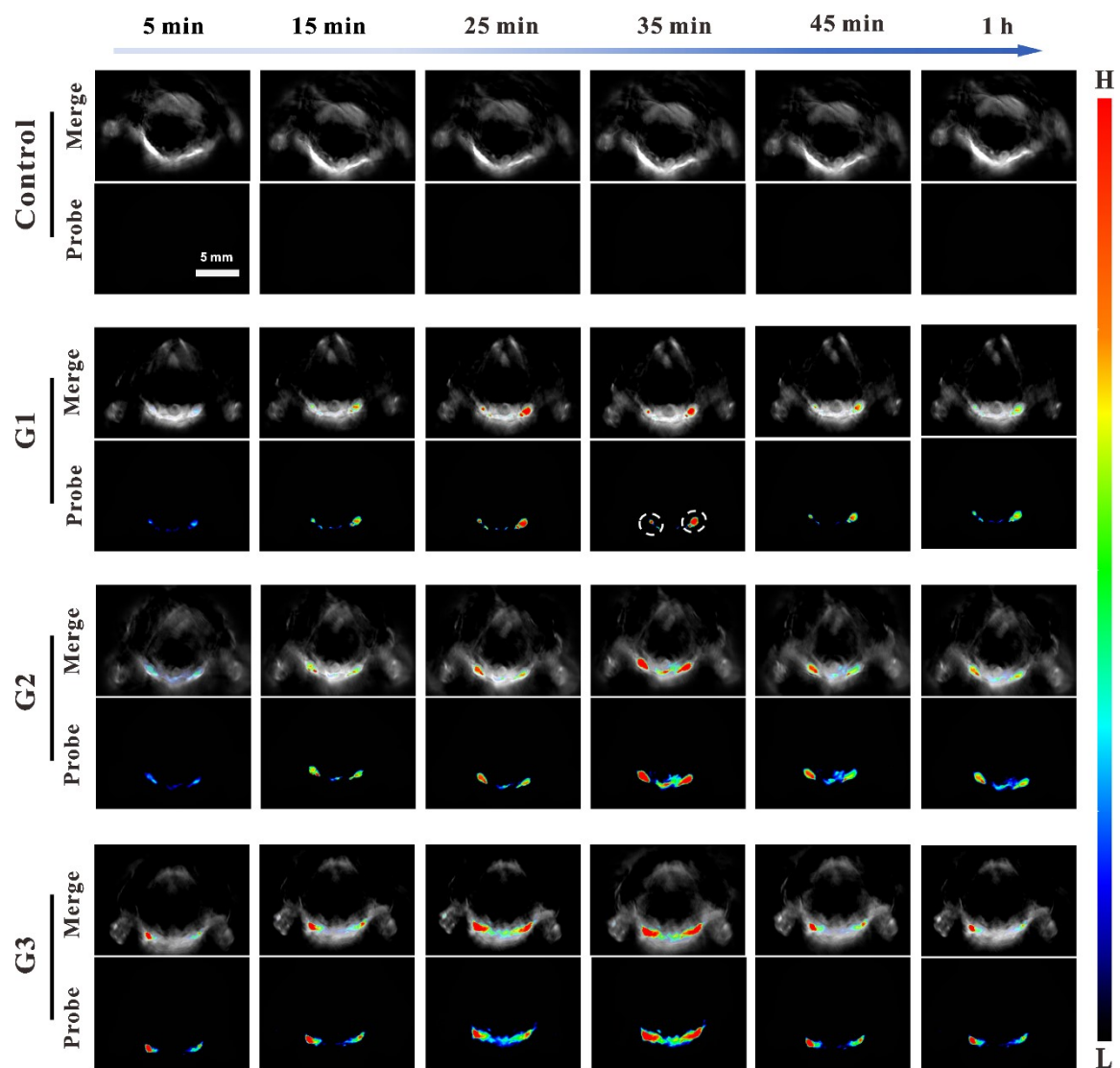


Figure S13 Cross-sectional MSOT images of the different groups of mice injected with the probe HCD9-Zn[II] (3.2 mg kg^{-1}) and after ATP pre-injection (Control: 0 mg kg^{-1} , G1: 0.5 mg kg^{-1} , G2: 1.1 mg kg^{-1} , G3: 2.2 mg kg^{-1}) (The white dotted-line circle ROI covering the jugular veins) Scale bar: 5 mm.

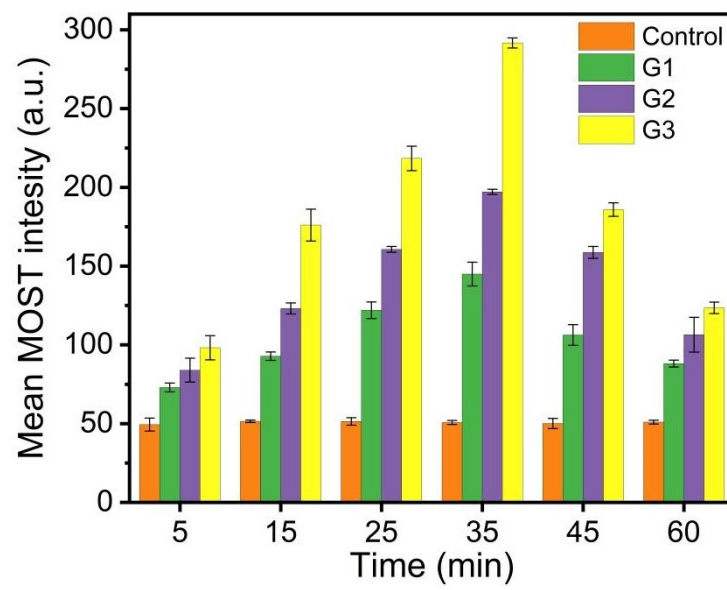


Figure S14 Mean MSOT intensities of the ROI covering the jugular veins (the white circle) at different time (n = 3).

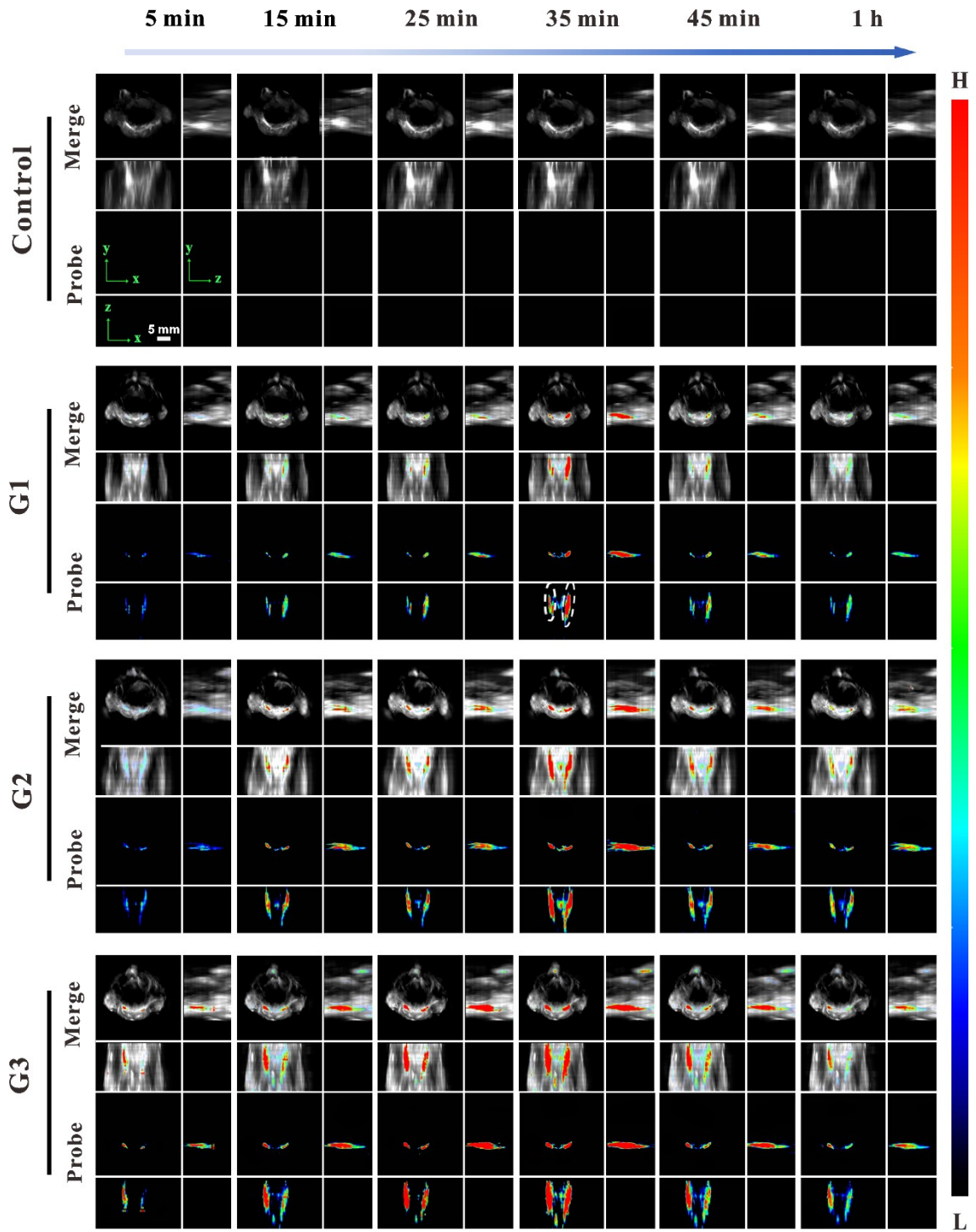


Figure S15 The 3D-MSOT images after the HCD9-Zn[II] injection (3.2 mg kg⁻¹) and after ATP pre-injection (Control: 0 mg kg⁻¹, G1: 0.5 mg kg⁻¹, G2: 1.1 mg kg⁻¹, G3: 2.2 mg kg⁻¹). Scale bar: 5 mm. In a 3D-MSOT image, x-y plane is presented in the top-left subpanel, y-z plane is in the top-right subpanel, and x-z plane is in the bottom-left subpanel. (The white dotted-line circle ROI covering the jugular veins).

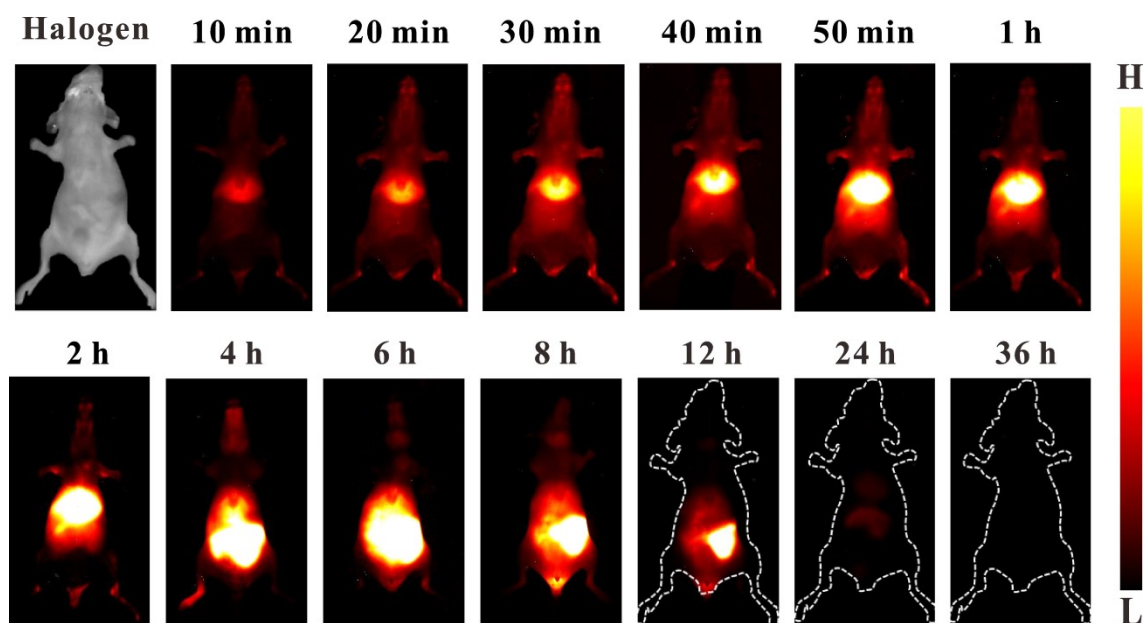
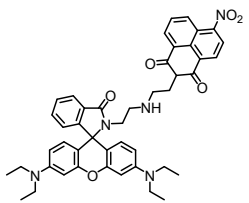
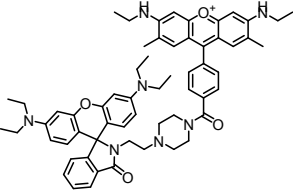
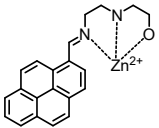
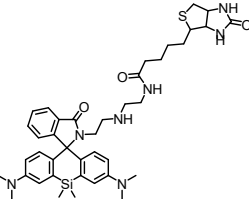
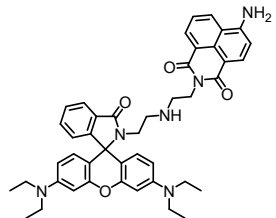
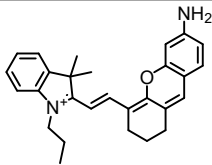
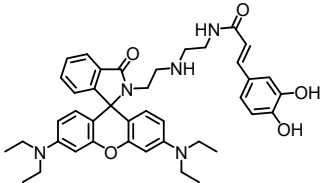
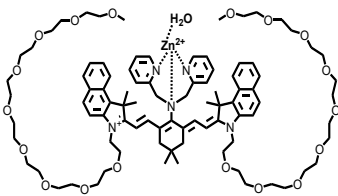


Figure S16 The NIR-II fluorescence images upon HCD9 injection in mice (3.2 mg kg^{-1}). 808 nm laser as excitation (50 mW cm^{-2}).

Table S1. Comparison of this probe with the literature-reported representative optical probes for ATP detection.

Fluorescent probe	Emission peak (nm)	Emission range (Visible light, NIR- I or NIR- II)	Detection limit (μM)	Response time	Imaging method	Samples for detection	Water soluble	Reference
	580	Visible light	50	5 min	Fluorescence imaging	Cells	No	[1]
	560/624	Visible light	4.65	200 s	Fluorescence imaging	Cells	No	[2]
	456	Visible light	0.0036	110 s	Fluorescence imaging	Cells	No	[3]
	675	Visible light	33.3	240 s	Fluorescence imaging	Cells, mice	No	[4]

	589	Visible light	2	10 min	Fluorescence imaging	Cells	No	[5]
	702	NIR-I	0.13	2 min	Fluorescence imaging	Cells, foods	No	[6]
	588	Visible light	14	23 min	Fluorescence imaging	Cells	No	[7]
	924	NIR-II	1.09	100 s	Fluorescence and optoacoustic imaging	Mice	Yes	This work

References:

- [1] Y Fang, W Shi, Y M Hu, X H Li, H M Ma, A dual-function fluorescent probe for monitoring the degrees of hypoxia in living cells via the imaging of nitroreductase and adenosine triphosphate, *Chem Commun.*, 2018, 54, 5454-5457.
- [2] T B Ren, S Y Wen, L Wang, P Lu, B Xiong, L Yuan, X B Zhang, Engineering a Reversible Fluorescent Probe for Real-Time Live-Cell Imaging and Quantification of Mitochondrial ATP, *Anal. Chem.*, 2020, 92, 4681-4688.
- [3] X P Zhang, J X Liu, J Wang, L Han, S T Ma, M Q Zhao, G L Xi. Adenosine triphosphate (ATP) and zinc(II) ions responsive pyrene based turn-on fluorescent probe and its application in live cell imaging. *J Photoch. Photobio. B*, 2021, 223, 112279.
- [4] W L Jiang, W Y Wang, Z Q Wang, M Tan, G J Mao, Y F Li, C Y Li. A tumor-targeting near-infrared fluorescent probe for real-time imaging ATP in cancer cells and mice, *Anal. Chim. Acta*, 2022, 1206, 339798.
- [5] L L Yao, W J Zhang, C X Yin, Y B Zhang, F J Huo, A tracer-type fluorescent probe for imaging adenosine triphosphate under the stresses of hydrogen sulfide and hydrogen peroxide in living cells, *Analyst*, 2022, 147, 4222-4227.
- [6] N Ding, M W Qin, Y H Sun, S Qi, X Z Dong, S Niazi, Y Zhang, Z P Wang, Universal Near-Infrared Fluorescent Nanoprobes for Detection and Real-Time Imaging of ATP in Real Food Samples, Living Cells, and Bacteria, *J. Agric. Food Chem.*, 2023, 71, 12070-12079.
- [7] J H Liu, W Zhang, X Wang, Q Ding, C C Wu, W Zhang, L L Wu, T D James, P Li, B Tang, Unveiling the Crucial Roles of $O_2^{\bullet-}$ and ATP in Hepatic Ischemia-Reperfusion Injury Using Dual-Color/Reversible Fluorescence Imaging, *J. Am. Chem. Soc.*, 2023, 145, 19662-19675.